Supporting Information

Photoinduced absorption and linear/nonlinear emission of assembled carbon dot-silica nanocomposites for cellular imaging

Jiangling He,*[a] Xu Chen,*[a] and Youling He *[b]

[a] National R&D Center for Se-rich Agricultural Products Processing, Hubei Engineering Research Center for Deep Processing of Green Se-rich Agricultural Products, School of Modern Industry for Selenium Science and Engineering, Wuhan Polytechnic University, Wuhan 430023, P. R. China. E-mail: hejiangling@whpu.edu.cn; chxu@whpu.edu.cn

[b] College of Physics and Optoelectronic Engineering, Shenzhen University, Shenzhen 518060, P. R. China. E-mail: heyouling@szu.edu.cn

1. Structural analysis of CDs:

FT-IR result indicates there are abundant functional groups on the surface of CDs as shown in **Figure S1**, including O-H/N-H, C-H, C=O, C-O/C-N etc. XPS survey reveals the atomic percentage of C, O, and N is 74.29%, 22.05%, and 3.66%, respectively. Fitting curves indicate C_{1s}, O_{1s}, and N_{1s} spectra can be fitted by various functional regions as shown in **Figure S2**. In **Figure S3**, the high-resolution TEM image demonstrates that CDs have the lattice fringe spacing of ~0.19 nm and ~0.21 nm, which are corresponding to (102) and (100) planes of the graphite, respectively [1, 2]. Such high carbon atomic content and structure result can further demonstrate the CDs were as-prepared successfully.

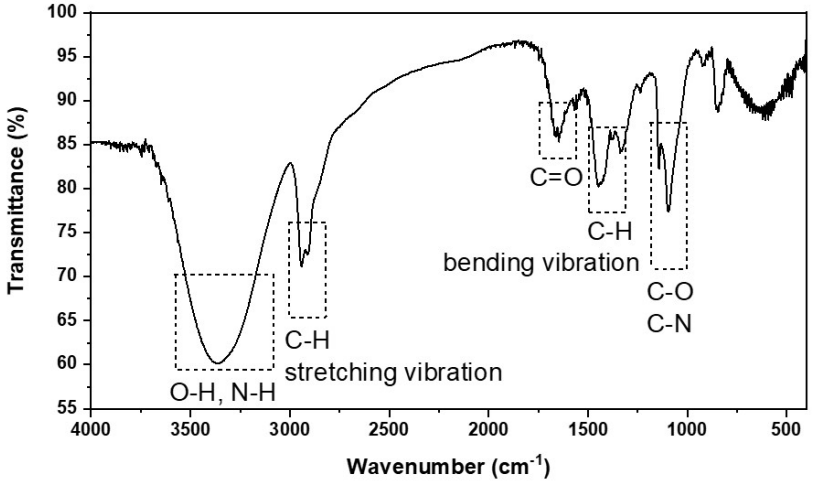

Figure S1. FT-IR spectrum of CDs.

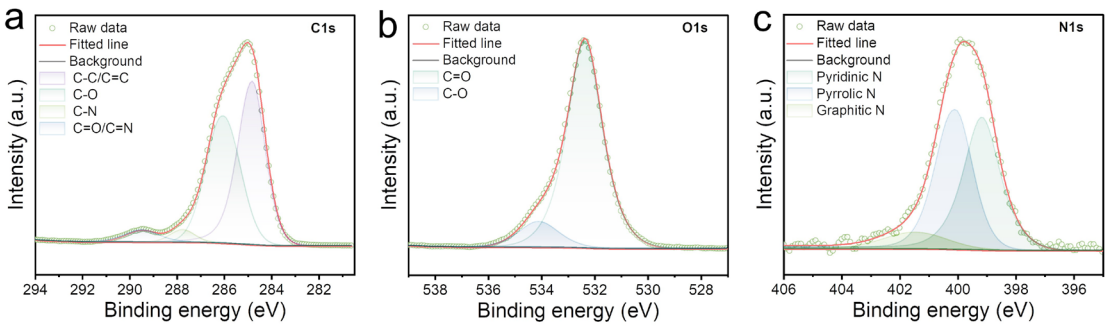

Figure S2. XPS results of CDs. (a-c) C_{1s} spectrum, O_{1s} spectrum, N_{1s} spectrum, and their corresponding fitting results, respectively.

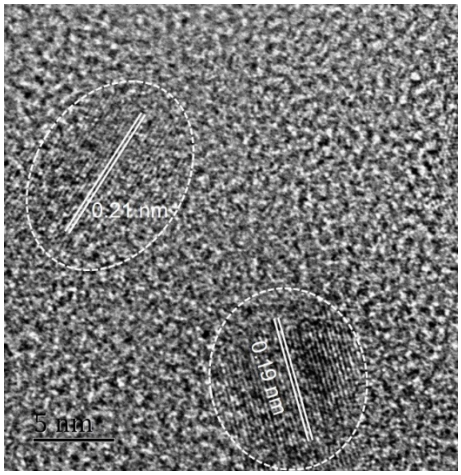

Figure S3. High-resolution TEM image of CDs.

2. Preparation Optimization, Structural analysis and Optical Property of CDs-SiO_2:

In the process of synthesizing the CDs-SiO_2 composite, we optimized the condition via adjusting the ratio between CDs and SiO_2. We set 5 experimental groups of 1 mg, 3 mg, 5 mg, 7 mg, and 9 mg of CDs respectively reacted with 2 mL of TEOS according to the preparation method as shown in the revised manuscript (**Figure S4**). We found that the group 3 has the optimal emission intensity under the excitation of 760 nm ultrafast femtosecond laser, indicating the sample from group 3 relatively has great potential in terms of nonlinear properties, so the group 3 was used as the research group.

The FTIR, XPS, and TEM image of CDs-SiO_2 were shown in **Figure S5-S7**, respectively. It can be seen that after the formation of CDs-SiO_2 composite, there are obvious new functional groups, mainly including Si-O-C, Si-C, and Si-O as shown in **Figure S5**. XPS results indicate that the atomic percentage of C, O, and Si is 14.63%, 57.52%, and 27.85%, respectively. Fitting curves also indicate C_{1s}, O_{1s}, and Si_{2p} spectra can be fitted by various functional regions as shown in **Figure S6**.

Comparing it with the XPS results of CDs proves the new formation of Si-O-C and SiO_2 bonds for CDs-SiO_2. These results further confirm that CDs are anchored onto silica via Si-O-C functional groups. (HR)TEM images of as-prepared CDs-SiO_2 are shown in **Figure S7**. In addition, we also measured the DLS of CDs and CDs-SiO_2. However, the DLS of CDs was failed to be gathered due to the quite small size of CDs, and that of CDs-SiO_2 was shown in **Figure S8**, which demonstrates the size distribution of this composite was mainly located at ~20 nm. The fitting results for the UV-Vis absorption spectrum of CDs-SiO_2 were shown in **Figure S9**. Due to the peak at 252 nm was occurred and it should be contributed to π→π* transition from the C=C bonds, and another broad band with a shoulder at 348 nm was from C=O bonds, resulting from the n→π* transition process [3-5]. Thus the weak shoulder at the peak of 280 nm was mainly occurred by n→π* transition from the C=O bonds. It was measured that the fluorescence intensity and phosphorescence intensity of CDs-SiO_2 composite within the storage of 30 days as shown in **Figure S10**. Both the fluorescence and phosphorescence signals were quite stable, indicating as-obtained CDs-SiO_2 composite has high PL stability.

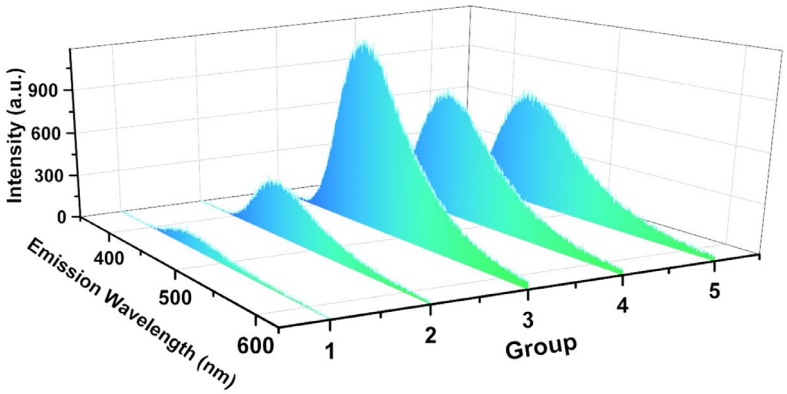

Figure S4. The emission spectra of as-prepared composites with various ratios under the excitation of 760 nm ultrafast femtosecond laser (group 1-5: 1 mg, 3 mg, 5 mg, 7 mg, and 9 mg of CDs reacted with 2 mL of TEOS, respectively.

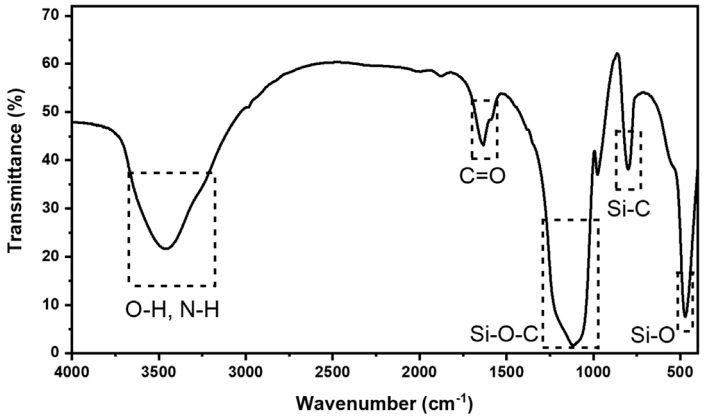

Figure S5. FT-IR spectrum of CDs-SiO_2.

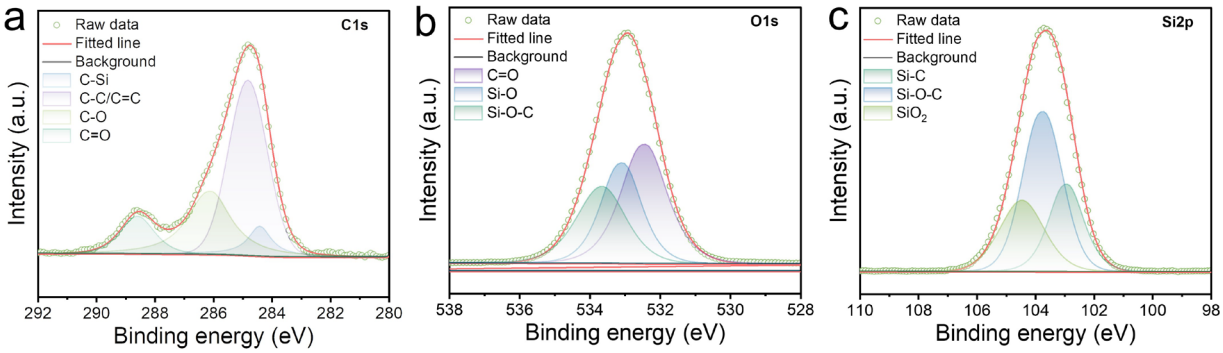

Figure S6. XPS results of CDs-SiO_2. (a-c) C_{1s} spectrum, O_{1s} spectrum, Si_{2p} spectrum, and their corresponding fitting regions, respectively.

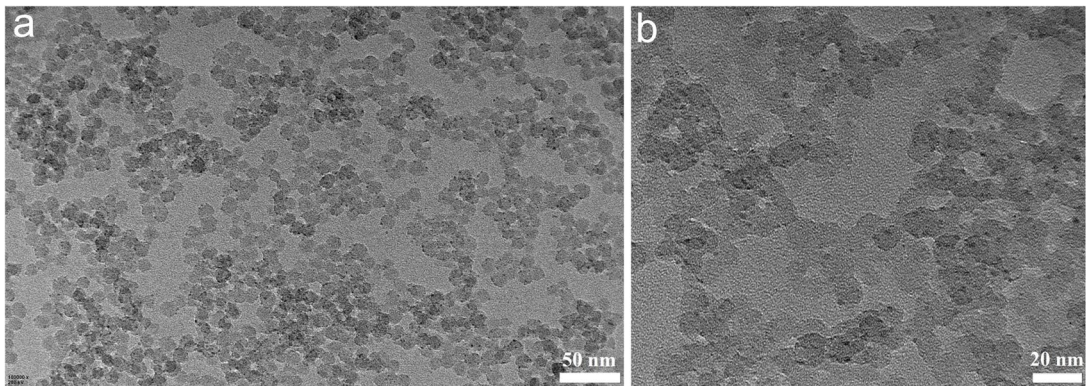

Figure S7. (a) TEM image and (b) High-resolution TEM image of CDs-SiO_2.

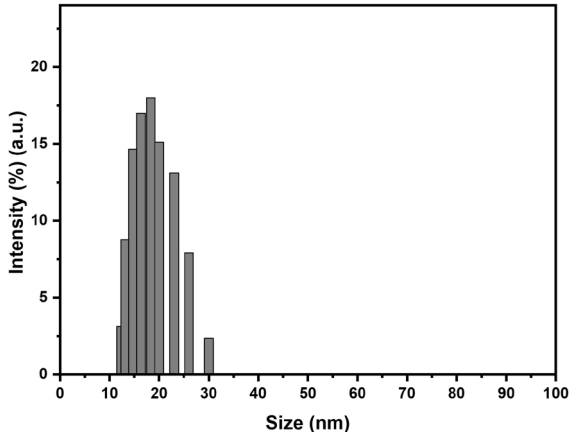

Figure S8. Size distribution of CDs-SiO_2 via DLS measurement.

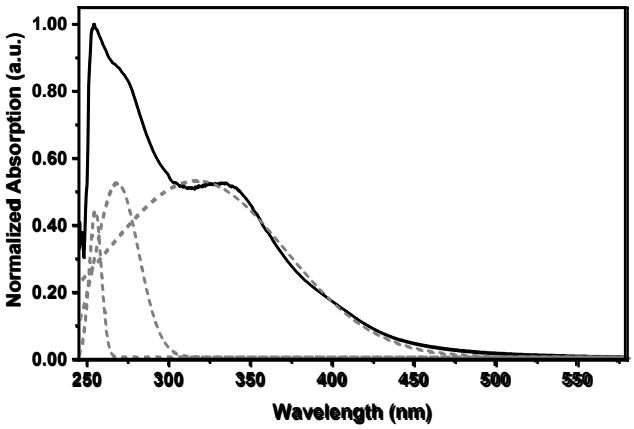

Figure S9. The fitting curves for the absorption spectrum of CDs-SiO_2.

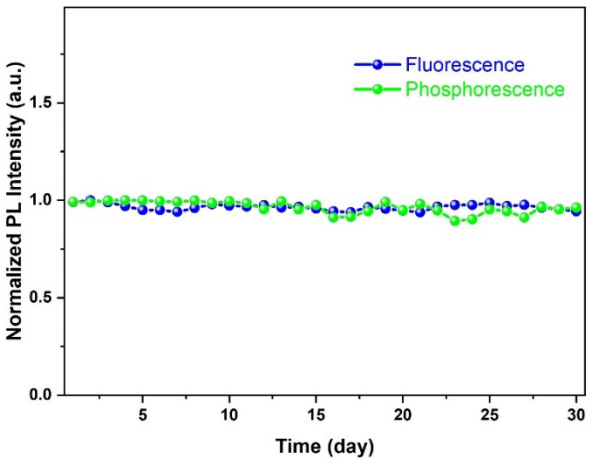

Figure S10. The normalized PL intensity of CDs-SiO_2 within the storage of 30 days.

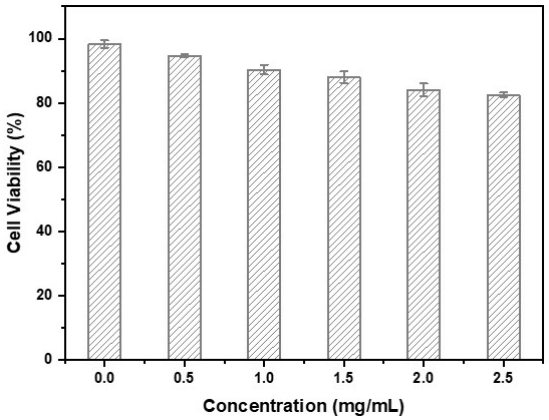

Figure S11. Viability of HeLa cells incubated with CDs-SiO_2 in the range of 0-2.5 mg/mL.

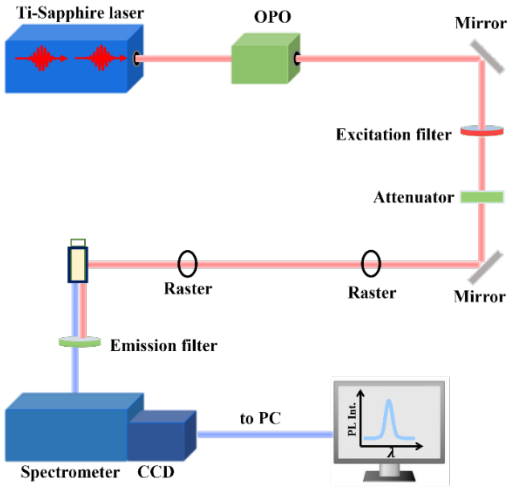

Figure S12. Optical route for the 2PEF spectra measurement.

Table S1. Average lifetime of CDs-SiO_2 composite under various temperatures and the percentage distribution of Phos. and TADF components (monitored at 418 nm).

Temp. (K)	$\tau_{1,TADF}$ (ms)	(%)	$\tau_{2,TADF}$ (ms)	(%)	$\tau_{3,Phos.}$ (ms)	(%)	TADF (%)	Phos. (%)	$\tau_{ave.}$(ms)
84.09	15.4056	4.07	385.6932	11.43	3778.4518	84.50	15.50	84.50	3237.5
120.0	16.4919	4.58	293.1283	10.72	3170.0281	84.70	15.30	84.70	2717.2
200.0	18.3685	4.37	326.8768	12.51	3158.4143	83.12	16.88	83.12	2667.0
240.0	25.9962	3.74	463.0941	18.35	2665.6262	77.91	22.09	77.91	2163.0
280.0	46.3474	5.11	399.0243	26.39	2196.6585	68.50	31.50	68.50	1612.4
298.0	28.4243	5.72	254.6932	22.42	1430.9830	71.85	28.15	71.85	1086.9
320.0	14.3699	5.85	145.7345	22.79	883.8883	71.35	28.65	71.35	664.70
400.0	16.2782	28.20	78.7044	55.73	511.3113	16.08	83.92	16.08	130.67
440.2	13.7426	53.03	63.4594	36.74	386.4117	10.23	89.77	10.23	70.133
480.1	9.1645	66.89	57.4183	22.40	283.3770	10.71	89.29	10.71	49.342

References:

1. W. Fan, J. He, H. Wei, C. Zhang, M. Zhu, D. Xu, S. Xiao, J. He, Z. Chen and J. Meng, *Results Phys.*, 2022, **38**, 105591.
2. Y. He, J. He, L. Wang, Z. Yu, H. Zhang, Y. Liu and B. Lei, *Sens. Actuators, B*, 2017, **251**, 918-926.
3. J. He, Y. He, Y. Chen, X. Zhang, C. Hu, J. Zhuang, B. Lei and Y. Liu, *Chem. Eng. J.*, 2018, **347**, 505-513.
4. Y. Sun, J. Liu, X. Pang, X. Zhang, J. Zhuang, H. Zhang, C. Hu, M. Zheng, B. Lei and Y. Liu, *J. Mater. Chem. C*, 2020, **8**, 5744-5751.
5. Y. Sun, S. Liu, L. Sun, S. Wu, G. Hu, X. Pang, A. T. Smith, C. Hu, S. Zeng, W. Wang, Y. Liu and M. Zheng, *Nat. Commun.*, 2020, **11**, 5591.